Effects of Stabilizer Thickness of 2G HTS Wire on the Design of a 1.5-MW-Class HTS Synchronous Machine

Article *in* IEEE Transactions on Applied Superconductivity · June 2016

DOI: 10.1109/TASC.2016.2549547

CITATIONS
9

READS
211

10 authors, including:

Ji Hyung Kim
Jeju National University
140 PUBLICATIONS **1,861** CITATIONS
SEE PROFILE

Thanh-Dung Le
University of Luxembourg
38 PUBLICATIONS **250** CITATIONS
SEE PROFILE

Young-Sik Jo
Korea Electrotechnology Research Institute-KERI
84 PUBLICATIONS **863** CITATIONS
SEE PROFILE

Yong-Soo Yoon
Shin Ansan University
148 PUBLICATIONS **1,314** CITATIONS
SEE PROFILE

Effects of Stabilizer Thickness of 2G HTS Wire on the Design of a 1.5-MW-Class HTS Synchronous Machine

Ji Hyung Kim, Thanh Dung Le, Do Jin Kim, Chang-Jin Boo, Young-Sik Jo, Yong Soo Yoon, Kyung Yong Yoon, Yoon Hyuck Choi, Haigun Lee, and Ho Min Kim

***Abstract*—In general, a metallic stabilization layer is overcoated on the outermost layer of a second-generation high-temperature superconducting (2G HTS) wire to stably transfer current against thermal and magnetic disturbances. Stabilizer thickness T_s is one of the key issues in an HTS synchronous machine (HTSSM) application because it strongly affects the electrical output performance of the machine and the stable operation and reliable protection of the HTS field coil. In this paper, a design and characteristic analysis for manufacturing a 1.5-MW-class HTSSM was performed using a 2-D analytical design code and a 3-D finite-element method. Various T_s values were considered in the HTS field-coil design to investigate their effects on the stability and protection of the HTS coil and the back-electromotive force of the machine. The design parameters are also discussed to determine suitable T_s for the 2G HTS wire.**

***Index Terms*—Adiabatic superconducting magnets, Cu stabilizer thickness, heating duration, phase back-electromotive force, stability margin.**

I. Introduction

COMMERCIALIZED second-generation high-temperature superconducting (2G HTS) wires are generally manufactured in the form of a composite conductor by laminating a metallic layer of a so-called stabilizer such as copper (Cu), stainless steel, or silver on the outermost layer of the wire. The 2G HTS wire plays a significant role in the stable transfer of a DC transport current from a superconducting layer, i.e., (RE) BCO layer, to a metallic layer under thermally and magnetically unstable operating conditions of HTS magnets and in providing mechanical strength and thermal conduction [1], [2]. If a hotspot caused by transitory or prolonged magnetic, thermal, or mechanical disturbance occurs in the local-region (RE) BCO layer of a composite conductor, most of the charged DC currents and generated thermal heat are bypassed and transferred to a stabilizer with a proper thickness.

The thickness of the stabilization layer for a 2G HTS wire is one of the key issues in an HTS synchronous machine (HTSSM) application because it technically affects the electrical output performance of the rotating machine and the operating and protection characteristics of the HTS field coil.

The present study focuses on three effects of the changes in the stabilizer thickness (T_s) of the 2G HTS wire in terms of electrical output performance of a rotating machine and the stability and protection issues of HTS field coils. Therefore, in this study, we developed a comparative design of a 1.5-MW-class HTSSM considering different T_s values of the wire for HTS field coils. First, electromagnetic finite element method (FEM) analyses were conducted to calculate the phase back-electromotive force (EMF) of a 1.5-MW-class HTSSM. We then studied the stability and protection characteristics of HTS field magnets according to the FEM simulation results. Finally, comparative analysis results were presented and discussed to determine a suitable T_s value of the 2G HTS wire.

II. Effects of Stabilizer Thickness of HTS Wire on the Machine Characteristics

A. Effects of Changes in Stabilizer Thickness

Fig. 1 shows the influence of various T_s values of an HTS wire on the output performance of the HTSSM and the stability and protection of the HTS field coils. The conductor current density $(J_{\rm cd})$, matrix current density (J_m), and winding pack current density $(J_{\rm wd})$ of the HTS field coil vary according to the changes in T_s of the HTS wire. The crucial electromagnetic design parameters such as phase back- EMF of the HTSSM, maximum magnetic field density $(B_{\rm mag})$, maximum magnetic field perpendicularly applied to the tape (B_p), stored energy (W), and inductance (L) of the HTS coil depend on the $J_{\rm wd}$ value of the field coil, which varies with T_s. In addition, the temperature margin $(\Delta T_{\rm op})$ and stability margin (Δe_h), which may indicate the HTS coil stability, are affected by the B_p value caused by changes in T_s. Finally, some parameters in

Manuscript received October 20, 2015; accepted March 30, 2016. Date of publication April 1, 2016; date of current version May 23, 2016. This work was supported by the 2016 scientific promotion program funded by Jeju National University.

J. H. Kim, T. D. Le, D. J. Kim, and H. M. Kim are with the Department of Electrical Engineering, Jeju National University, Jeju 63243, South Korea (e-mail: hmkim@jejunu.ac.kr).

C.-J. Boo is with the Department of Electrical Engineering and Energy, Jeju International University, Jeju 63309, South Korea.

Y.-S. Jo is with the Korea Electrotechnology Research Institute, Changwon 51543, South Korea.

Y. S. Yoon is with the Department of Electrical Engineering, Shin Ansan University, Ansan 15435, South Korea.

K. Y. Yoon is with the Department of Electrical and Electronic Engineering, Yonsei University, Seoul 03722, South Korea.

Y. H. Choi and H. Lee are with the Department of Materials Science and Engineering, Korea University, Seoul 02841, South Korea.

Color versions of one or more of the figures in this paper are available online at http://ieeexplore.ieee.org.

Digital Object Identifier 10.1109/TASC.2016.2549547

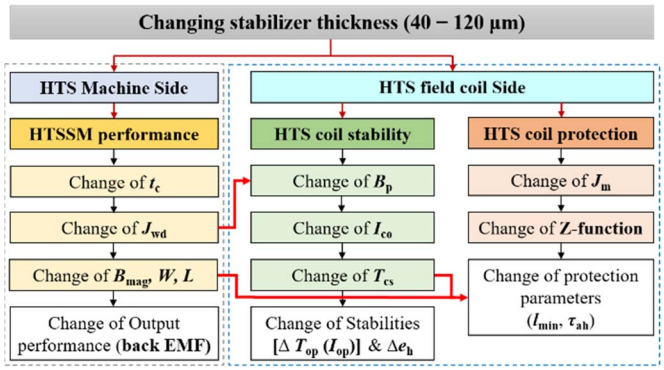

Fig. 1. Effects of the stabilizer thickness of an HTS wire on the stability and protection of HTS field coils and HTSSM performance.

TABLE I
MAJOR SPECIFICATIONS OF THE COMMERCIAL 2G HTS WIRE FOR THE FIVE DESIGNS

Items	Unit	Values
Conductor type		(RE) BCO coated conductor
Width	[mm]	12
Thickness	[mm]	0.07–0.18
REBCO Thickness T_{re}	[μm]	1–2 (in 2014)
Stabilizer thickness T_s	[μm]	40#, 10–120## (both sides)
Min. I_c @77 K, self-field	[A]	300
Stabilizer material		Copper

#: standard product, ##: special order product

the design of the HTS coil protection scheme, including the minimum normal zone length $(l_{\min})$ and heating duration (τ_{ah}), are influenced by J_m. Therefore, various T_s values should be cautiously considered and properly applied in the HTSSM development.

B. Commercial 2G HTS Wire

A surround Cu stabilizer (SCS) 12050 advanced pinning (AP) type, which can be commercially produced and ordered from SuperPower Inc. (SPI), was selected as the wire for the HTS field coils. The various major specifications of the 2G HTS wire for five design models are listed in Table I. This wire has been manufactured with 12-mm width and 0.07–0.18-mm thickness and is surrounded by a Cu stabilization layer of 0.01–0.12 mm on both outermost sides of the wire. Stabilizer thickness T_s of 0.04 mm is standard for certain products, and others are used for special-order products. The critical current (I_c) was 300 A, generated at a 77-K operating temperature under a self-field condition [3].

III. PERFORMANCE OF HTSSM

A. Conceptual Design of the HTS Field Coil

The machine design parameters were specified in [4], which focused on the conceptual electromagnetic design of a 1.5-MW-class HTSSM. Fig. 2 shows a cross-sectional view of a conceptual design for a 1.5-MW-class HTSSM and the HTS field-coil design view considering the T_s values of the wire. The structure contains a mechanical shield, armature coils, a flux damper, a cryostat, and an HTS field coil. Fig. 2(b) shows the zoom-out view of the basic structure of an HTS single pancake

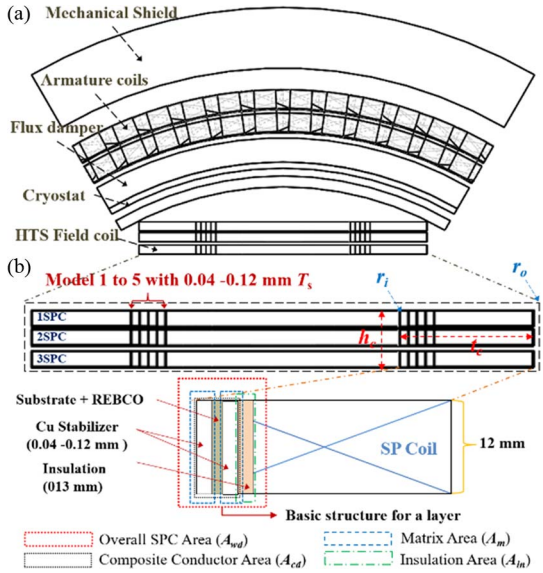

Fig. 2. (a) Cross-sectional view of a one-sixth design of a 1.5-MW-class HTSSM. (b) HTS field-coil view with the mentioned parameters.

TABLE II
HTS FIELD-COIL DESIGN PARAMETERS CONSIDERING THE STABILIZER THICKNESS

Items	Unit	Model 1	Model 2	Model 3	Model 4	Model 5
				Values		
T	[mm]	0.1	0.12	0.14	0.16	0.18
T_s	[mm]	0.04	0.06	0.08	0.1	0.12
T_i	[mm]	0.13				
l_s	[mm]	635				
l_t	[mm]	1006				
h_c	[mm]	42				
t_c	[mm]	73.37	79.75	86.13	92.51	98.89
r_i	[mm]	112.09	105.71	99.33	92.95	86.57
r_o	[mm]	185.46				
J_{cd}	[A/mm^2]	254.17	211.81	181.55	158.85	141.20
J_m	[A/mm^2]	635.42	423.61	317.71	254.17	211.81
J_{wd}	[A/mm^2]	110.51	101.67	94.14	87.64	81.99
F_{co}	[%]	43.48	48	51.85	55.17	58.07
α	[r_o/r_i]	1.65	1.75	1.87	2.0	2.14
I_{op}	[A]	305				
N_c		957				
MMF	[AT]	291885				
l_w	[m]	12660	12545	12430	12315	12199

T: wire thickness, T_i: insulation thickness, l_s: axial length, l_t: total coil length, h_c: height of SPCs, t_c: thickness of SPCs, F_{co}: coil filling factor, N_c: winding turns per pole

coil (SPC) with the parameter definitions. An electromagnetic air-gap size of 63 mm and the magnetomotive force (MMF) values of the HTS field coil were set as constant to obtain comparable analysis results under equivalent design conditions. Table II lists the HTS field-coil parameters of five models, which were built up by CAD software for 3D FEM simulations. To investigate some effects of T_s of a 2G HTS wire on the characteristics of machine performance and stability as well as on the protection of the HTS field coil, we used HTS wires in the field-coil windings in this study with T_s values ranging from 0.04 to 0.12 mm. A T_s value below 0.04 mm is not effective in enhancing the stability and protection of the HTS field coil. As mentioned in Section II-A, the J_{cd}, J_m, and, J_{wd} values of each analysis model were varied according to the changes in T_s.

Moreover, the inner radius of the field coil (r_i) in each model decreased because of the added stabilizer in the wire

TABLE III
THREE-DIMENSIONAL FEM ANALYSIS RESULTS FOR THE FIVE HTSSM DESIGNS

Items	Unit	Model 1	Model 2	Model 3	Model 4	Model 5
				Values		
HTS Synchronous Rotating Machine						
Back EMF	[V_{rms}]	1874	1834	1790	1746	1698
HTS Field Coil						
Max. B_{mag}	[T]	2.74	2.64	2.53	2.5	2.45
Max. B_p	[T]	1.94	1.84	1.73	1.62	1.54
W	[J]	51258	48955	46677	44693	42712
L	[H]	1.1	1.05	1	0.96	0.92
C–P ratio†	[$/kAm]	77	80	81	83	86
HTS cost	[$]	894429	943384	991293	103815	108381

†:@operating condition

and the limitation in the outer radius (r_o) of the field coil. As T_s was further increased, the shape factor $\alpha(r_o/r_i)$ of the field coils also increased. As a result, the HTS SPC became thicker, meaning that the mechanical stress increased [5]. Accordingly, increasing T_s in terms of the mechanical strength of an HTS coil is counterproductive. Additionally, a significant softening effect of the stress–strain characteristic relationships for the SPI SCS-AP model occurs with additional Cu T_s due to the decreased modulus and yielding of the Cu material [6].

The larger the T_s value is, the lower is the required HTS wire length (l_w) in each model because r_i, i.e., the bending inner radius of the round part in a racetrack-type field coil, decreased with increasing T_s.

B. 3D FEM Analysis of Machine Performance

From [7], the output performance of an HTSSM, i.e., the phase back-EMF, is sensitively affected by $B_{\rm mag}$ of the rotor HTS field coil, which determines the degree of the coupled linkage flux in air-core armature windings and is directly proportional to the overall current density $(J_{\rm wd})$ of the winding pack in the HTS field coil. $J_{\rm wd}$ is expressed as [8], [9]

$$J_{\rm wd}=\frac{NI_{\rm op}}{(A_{\rm cd}+A_m+A_{\rm in})}=\frac{NI_{\rm op}}{A_{\rm wd}}=\frac{NI_{\rm op}}{h_c t_c}=\frac{NI_{\rm op}}{h_c(r_o-r_i)} \quad (1)$$

where $A_{\rm cd}$, A_m, and $A_{\rm in}$ are the cross-sectional areas of the composite conductor, matrix corresponding to the metallic stabilizer of the 2G wire, and insulation layer, respectively. Moreover, $A_{\rm wd}$ is the overall cross-sectional area of the SPC, which depends on the $A_m(T_s)$ value of the HTS wire, as shown in Fig. 2. Finally, $NI_{\rm op}$ is the MMF value of the HTS field coil, which is often called the total ampere-turns. In case of the same $NI_{\rm op}$ and h_c values, $J_{\rm wd}$ is inversely proportional to t_c, which can be changed by T_s.

Table III lists a summary of the 3D electromagnetic FEM analysis results considering the five field-coil designs with different Cu T_s values. These were obtained via ANSYS Maxwell 3D software which were used for the simulation in a time-transient solver for steady state of a motor no-load operation with fully charged $I_{\rm op}$ of 305 A and rated rotating speed of 200 rpm. Fig. 3 shows the steady-state waveform of the generated phase B back-EMF for the no-load operation with three cycles (300 ms). The $B_{\rm mag}$ and B_p values generated in the HTS SPCs for each model were computed at a range from 2.74 to

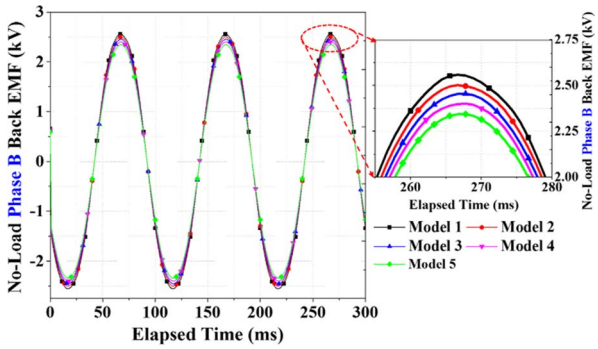

Fig. 3. Generated back-EMF of phase B in steady state for the no-load operation.

2.45 T and from 1.94 to 1.54 T, respectively. Consequently, the back-EMF values of each model were reduced from 1874 to 1698 $V_{\rm rms}$, as shown in Fig. 3. The back-EMF of the HTSSM and both magnetic field density values of the HTS field coil were inversely proportional to the increased Cu T_s, which may reduce the $J_{\rm wd}$ values. In addition, the coil W and L per pole were calculated as listed in Table III. These values are dependent not only on $B_{\rm mag}$ but also on the structural dimensions of the coil changed by the T_s value. The critical current values under the operating condition $(I_{\rm co})$ were estimated from the in-field properties under a 30-K cooling temperature and respective B_p values [3]. Model 5, with T_s of 0.12 mm, yielded the highest $I_{\rm co}$ value; hence, it will be more stable than the other models under the same disturbance conditions. Finally, the total costs of the required HTS wires to manufacture the HTS field coils were estimated using the unit cost (in dollars per meter) of the HTS wires, as listed in Table III [4]. The unit costs of each design model included the extra cost of added T_s and were supplied by SPI. Besides, the specific C–P ratios of all models were considered under the operating conditions based on the 3D FEM simulation results.

IV. STABILITY OF THE HTS FIELD COILS

Designing and manufacturing HTS magnets with robust stability require fundamental countermeasures such as avoiding thermal quench rather than merely protecting against it. Therefore, investigating the stability characteristics of HTS coils is necessary. Generally, HTS magnets can be categorized as adiabatic superconducting magnets of essentially five types, which can be classified by one of the cryostatic and adiabatic stability approaches [10], [11].

This section presents the so-called "stability margin" or "enthalpy margin" (Δe_h) estimated by an adiabatic stability approach to ensure reliable and stable operation of the HTS field coil [12]. Δe_h is the maximum permissible thermal energy density that must be absorbed by the volumetric enthalpy of the composite conductor to maintain stable operation of the HTS magnet against various disturbances. If the disturbance energy density does not exceed Δe_h, the HTS magnet is thermally stable, at least during the DC-charging operation. However, HTS magnets applied to the field coil of HTSSMs occasionally operate in both magnetically asynchronous transient conditions such as coil charging and discharging, rotor startup, and load

TABLE IV
ESTIMATION RESULTS OF THE TEMPERATURE AND STABILITY MARGIN OF HTS FIELD COILS FOR THE FIVE HTSSM DESIGNS

Items	Unit	Model 1	Model 2	Model 3	Model 4	Model 5
				Values		
I_{co} †	[A]	913	940	979	1012	1033
Lift factor ‡		3.04	3.13	3.26	3.37	3.44
i_{op}	[I_{op}/I_{co}]	0.334	0.324	0.312	0.301	0.295
T_c	[K]	86.9	87.2	87.4	87.5	87.7
$T_{cs}(I_{op})$	[K]	67.89	68.64	69.52	70.17	70.66
$[\Delta T_{op}]$	[K]	37.89	38.64	39.52	40.17	40.66
Δe_h	[J/cm^3]	31.434	32.547	33.875	34.871	35.631

†@30 K, Max. B_pT, ‡: [I_c (30 K, Max. B_p T)/I_c (77 K, self-field)]

fluctuations, as well as in thermally labile operating conditions. Thus, external disturbances acting on the HTS magnets might generate magnetically and thermally severe operating conditions. Therefore, vital HTS field coils should be designed with ample temperature and stability margins that consider external disturbances against permanent damage from local quench.

Sometimes, on behalf of Δe_h, a "temperature margin" $[T_{op}(I_{op})]$, which is the temperature deviation between the "current-sharing" temperature that depends on I_{op} and $T_{cs}(I_{op})$, and operating temperature $T_{op} = 30$ K can be used to define the level of stability. $[\Delta T_{op}(I_{op})]$ can be easily calculated by [11]

$$[\Delta T_{op}(I_{op})] = T_{cs}(I_{op}) - T_{op} = (T_c - T_{op})(1 - i_{op}) \quad (2)$$

where T_c is the critical temperature of an YBCO wire given by the maximum B_p values of each model as listed in Table IV and i_{op} is the I_{op} margin defined as the ratio of I_{op} to I_{co}. Note that if T_{op} and I_{op} are kept constant, $[\Delta T_{op}(I_{op})]$ is dominantly dependent on the I_{co} value affected by Cu T_s, as mentioned in Section II.

Under adiabatic conditions, Δe_h is based on the energy balance of the power density equation governing the thermal behavior of the superconductor and simply expressed as [12]

$$\Delta e_h = \int_{T_{op}}^{T_{cs}(I_{op})=T_{op}+[\Delta T_{op}(I_{op})]} C_{cd}(T)dT \quad (3)$$

where $C_{cd}(T)$ is the temperature-dependent heat capacity per unit volume of a composite conductor.

Table IV lists the results of estimated $[\Delta T_{op}(I_{op})]$ and Δe_h of the five case models with different Cu T_s values. Specifically, we assume that the selected material for the stabilizer of the SCS12050-AP-type 2G HTS wire used in this design is Cu (RRR 100), and the corresponding heat capacity is substituted for $C_{cd}(T)$ of the composite HTS wire in (3) [10], [13].

Fig. 4 shows the I_{co} versus temperature plots of the five models. As T_s increases, i_{op} is reduced by increasing I_{co}; thus, $[\Delta T_{op}(I_{op})]$ increases. Model 5 with a 0.12-mm T_s has the largest $[\Delta T_{op}(I_{op})]$ value at 40.66 K. Fig. 5 shows the temperature-dependent volumetric enthalpy energy profile of Cu (RRR 100) obtained from T_{op} and $T_{cs}(I_{op})$ in each model. For each model, the Δe_h value varies from 31.434 to 35.631 J/cm^3, which is shown in Fig. 5.

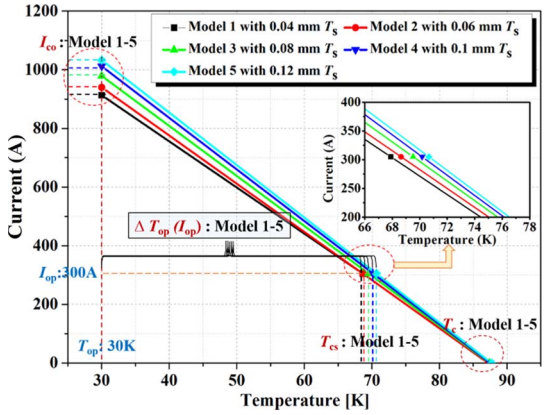

Fig. 4. Comparison of I_{co} versus temperature plots for the five models.

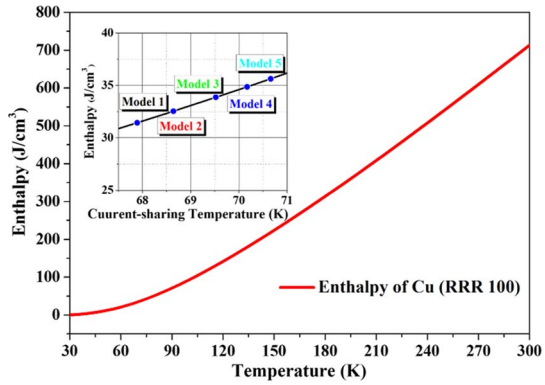

Fig. 5. Temperature-dependent volumetric enthalpy profile of Cu (RRR 100).

V. PROTECTION OF THE HTS FIELD COILS

When a quench occurs in the superconducting coils, the purpose of the protection operation is to restrain temperature increases in the hotspots in arbitrary local points, which could lead to permanent damage of the superconducting coils from burnout. The active protection technique should be better to protect the HTS coils than the passive technique, self-protection owing to high stability, and very slow normal zone propagation velocities (NZPV) of the HTS. Besides, choosing an appropriate protection scheme in both the active protection techniques for the HTS coils such as the detect-and-dump and detect-and-activate-heater protections is important. However, prior to designing the protection scheme, the possibility of protection for the designed HTS coil must be determined, especially in large HTS coils with high I_{op}.

Heating duration (τ_{ah}) refers to the time needed after quench or starting current sharing for the temperature of the local hotspot to rise from the initial temperature $(T_i = T_{op})$ to the final temperature (T_f), i.e., the permissible temperature level of the 2G wire under an adiabatic cryogenic condition. $\tau_{ah}(T_f, T_i)$ may be estimated by [14]–[16]

$$\tau_{ah}(T_f, T_i) = \left(\frac{A_{cd}}{A_m}\right) \frac{1}{J_m^2} \int_{T_i}^{T_f} \frac{C_m(T)}{\rho_m(T)} dT \quad (4)$$

$$= \left(\frac{A_{cd}}{A_m}\right) \frac{Z(T_f, T_i)}{J_m^2} \quad (5)$$

TABLE V
ESTIMATION RESULTS OF THE PROTECTION PARAMETERS FOR THE HTS FIELD COILS OF THE FIVE HTSSM DESIGNS

Items	Unit	Model 1	Model 2	Model 3	Model 4	Model 5
				Values		
$l_{\min}$	[cm]	10.98	16.64	22.44	28.28	34.14
A_{cd}/A_m		2.5	2.0	1.75	1.6	1.5
J_m	[A/m^2]	63541	42361	31770	25416	21180
		6667	1111	8333	6667	5556
Z- function ($T_{300\,K}$, $T_{30\,K}$)	[10^{16}A^2 ·S/m^4]	13.5				
τ_{ah} ($T_{300\,K}$, $T_{30\,K}$)	[S]	0.81	1.47	2.28	3.26	4.40
$\Delta r^{\dagger}$	[mm]	73.37	79.75	86.13	92.51	98.89
NZPV‡	[mm/s]	1.0 (epoxy impregnation)				
τ_f	[S]	73.37	79.75	86.13	92.51	98.89

†: radial build ($r_o - r_i$), ‡: transverse direction

where J_m is the "matrix" current density defined as I_{op}/A_m. C_m and ρ_m are the heat capacity and resistivity of the matrix stabilizer, respectively. We assume that joule heating can be absorbed by the metallic stabilizer of the wire in the isolated adiabatic heating of a local hotspot without the conduction and cooling effects under a constant-current power supply mode operation of the HTS coil.

Because the J_m values in the current-sharing mode are calculated and changed by stabilizer thickness T_s, $\tau_{ah}(T_f, T_i)$ may be directly determined by T_s of the HTS wire. Therefore, we investigated $\tau_{ah}(T_f, T_i)$ according to the variations in T_s. T_i is the operating temperature (30 K), and T_f should be limited to below 300 K because the HTS coils are at risk when T_f exceeds 300 K. The value of Z-$(T_{300\,K}, T_{30\,K})$ was estimated at approximately 13.5×10^{16} A$^2 \cdot$ s/m^4 based on the temperature-dependent Z-(T_f, T_i) function curve of Cu (RRR 100) in [14], which depends only on the material properties.

Table V lists the estimation results of the protection parameters for the HTS field coils of the five models. We also calculated the minimum length of the normal zone $(l_{\min})$, which caused the quench, and a function of the T_{cs} and J_m values assuming 21.43-W/(cm $\cdot$ K) thermal conductivity and 0.00000002 $\Omega \cdot$ cm resistivity of (Cu RRR 100) at 30 K, respectively [17]. The calculated $l_{\min}$ value in a range from 11.56 to 35.67 cm was inversely proportional to each J_m^2 value. Thus, we conclude that $l_{\min}$ is predominantly dependent on T_s in this calculation. As a result, the $\tau_{ah}(T_{300\,K}, T_{30\,k})$ values were estimated from 0.81 to 4.4 s. When T_s in the HTS wire increased, $\tau_{ah}(T_f, T_i)$ and the final temperature caused by joule heating in the local hotspot can be prolonged and limited, respectively, because J_m is reduced by increasing T_s of the wire. We conclude that the stabilizer thickness should be added to the 2G HTS wire to allow a secure time needed to protect the HTS coils from burnout.

Moreover, we also simply calculate the full quench time (τ_f) at a very slow transverse NZPV of 1 mm/s [17]. The values of τ_f ranged from 73.37 to 98.89 s. Thus, the detect-and-dump technique is absolutely effective in protecting the HTS field coil of the five models.

VI. CONCLUSION

In this paper, the output performance of a 1.5-MW HTSSM using a 3D electromagnetic FEM tool that considered different Cu T_s has been presented. For the respective stabilizer thicknesses, both the stability and temperature margin of the HTS coil and other significant parameters related to designing a protection scheme were estimated based on the electromagnetic FEM analysis results and analytical methods.

In conclusion, adding the Cu T_s is appropriate in terms of stability and protection of HTS field coils. Model 5, with T_s of 0.12 mm, is the most effective for stable and reliable operation of the HTSSM in all models. However, it requires more 2G HTS wire to satisfy the target output power of a 1.5-MW-class HTSSM. Thus, it leads to a slight increase in the manufacturing cost of the field coil. A certain amount of economic feasibility must inevitably be traded off for commercialization of a technically reliable HTSSM.

REFERENCES

[1] N. Y. Kwon *et al.*, "The effects of a stabilizer thickness of the YBCO coated conductor (CC) on the quench/recovery characteristics," *IEEE Trans. Appl. Supercond.*, vol. 20, no. 3, pp. 1246–1249, Jun. 2010.

[2] N. Y. Kwon *et al.*, "Influence of stabilizer thickness on over-current test of YBCO-coated conductors," *Supercond. Sci. Technol.*, vol. 22, no. 4, Jan. 2009, Art. no. 045003.

[3] D. W. Hazelton, "2G HTS wire for demanding applications and continuous improvement plans," in *Proc. EUCAS*, Genova, Italy, Sep. 2013, pp. 1–26.

[4] J. H. Kim *et al.*, "Economic analysis of a 1.5-MW-class HTS synchronous machine considering various commercial 2G CC tapes," presented at the 24th International Conference on Magnet Technology (MT 24), Seoul, Korea, 2015.

[5] Y. Iwasa, *Case Studies in Superconducting Magnets: Design and Operational Issues*, 2nd ed. New York, NY, USA: Springer-Verlag, 2009, pp. 102–105.

[6] D. W. Hazelton, "SuperPower 2G HTS conductor," presented at the 1st Workshop on Accelerator Magnets in HTS (WAMHTS-1), Hamburg, Germany, May 21, 2014.

[7] J. H. Kim *et al.*, "Characteristic analysis of various structural shapes of superconducting field coils," *IEEE Trans. Appl. Supercond.*, vol. 25, no. 3, Jun. 2015, Art. no. 5201105.

[8] Y. Iwasa, *Case Studies in Superconducting Magnets: Design and Operational Issues*, 2nd ed. New York, NY, USA: Springer-Verlag, 2009, p. 115.

[9] Y. Iwasa, *Case Studies in Superconducting Magnets: Design and Operational Issues*, 2nd ed. New York, NY, USA: Springer-Verlag, 2009, p. 361.

[10] Y. Iwasa, "Stability and protection of superconducting magnets—A discussion," *IEEE Trans. Appl. Supercond.*, vol. 15, no. 2, pp. 2615–1620, Jun. 2005.

[11] Y. Iwasa *et al.*, "Stability and quench protection of coated YBCO 'composite' tape," *IEEE Trans. Appl. Supercond.*, vol. 15, no. 2, pp. 1683–1686, Jun. 2005.

[12] Y. Iwasa, *Case Studies in Superconducting Magnets: Design and Operational Issues*, 2nd ed. New York, NY, USA: Springer-Verlag, 2009, pp. 357–358.

[13] R. Wesche *et al.*, "HTS conductors for fusion: Thermal stability and quench," presented at the HTS^4 Fusion Conductor Workshop, Karlsruhe, Germany, May 26–27, 2011.

[14] Y. Iwasa, *Case Studies in Superconducting Magnets: Design and Operational Issues*, 2nd ed. New York, NY, USA: Springer-Verlag, 2009, pp. 469–473.

[15] S. Hahn *et al.*, "A 78-mm/7-T multi-width no-insulation ReBCO magnet: Key concept and magnet design," *IEEE Trans. Appl. Supercond.*, vol. 24, no. 3, Jun. 2014, Art. no. 4602705.

[16] W. Yao, J. Bascunan, S. Hahn, and Y. Iwasa, "MgB_2 coils for MRI applications," *IEEE Trans. Appl. Supercond.*, vol. 20, no. 3, pp. 756–759, Jun. 2010.

[17] W. S. Kim *et al.*, "Normal zone propagation in 2-dimensional YBCO winding pack models," *IEEE Trans. Appl. Supercond.*, vol. 18, no. 2, pp. 1249–1252, Jun. 2008.